

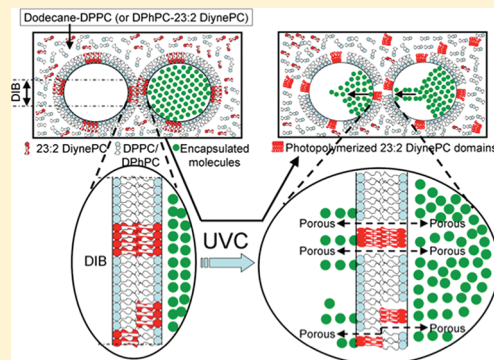
Triggered Release of Molecules across Droplet Interface Bilayer Lipid Membranes Using Photopolymerizable Lipids

S. Punnamaraju, H. You, and A. J. Steckl*

Nanoelectronics Laboratory, University of Cincinnati, Cincinnati, Ohio 45221, United States

Supporting Information

ABSTRACT: A combination of nonpolymerizable phospholipids (DPPC or DPhPC) and a smaller amount of cross-linking photopolymerizable phospholipids (23:2 DiynePC) is incorporated in an unsupported artificial lipid bilayer formed using the droplet interface bilayer (DIB) approach. The DIB is formed by contacting lipid monolayer-coated aqueous droplets against each other in a dodecane–lipid medium. Cross-linking of the photopolymerizable lipids incorporated in the DIB was obtained by exposure to UV–C radiation (254 nm), resulting in pore formation. The effect of cross-linking on the DIB properties was characterized optically by measuring the diffusion of selectively encapsulated dye molecules (calcein) from one droplet of the DIB to the other droplet. Changes in DIB conductivity due to UV–C exposure were investigated using current–voltage (*I*–*V*) measurements. The leakage of dye molecules across the DIB and the increase in DIB conductivity after UV–C exposure indicates the formation of membrane pores. The results indicate that the DIB approach offers a simple and flexible platform for studying phototriggered drug delivery systems *in vitro*.



I. INTRODUCTION

Phospholipids are key constituents of biological cellular membranes.¹ The phospholipid head groups are hydrophilic, while the fatty acid tails are hydrophobic. In aqueous environments, when two sheets of lipid monolayers come into contact with their hydrophobic tails facing each other, an artificial lipid bilayer can be formed. There are a wide range of artificial lipid bilayers, such as planar, supported, vesicles, and liposomes.² These artificial lipid bilayers have been applied to various biomimetic studies and applications.² A relatively recent approach for forming artificial lipid bilayers is the droplet interface bilayer (DIB). This approach involves dispensing aqueous droplets (with volumes ranging from picoliters to microliters) in an alkane bath containing a mixture of lipid molecules. The lipid molecules surround the aqueous droplets, with the headgroup in contact with the droplet and the tail remaining in the oil. When two lipid monolayer-coated droplets are brought into contact, they form a lipid bilayer at their interface. This idea originates from the earlier contributions by Tsosina et al.³ The first DIB was reported by Funakoshi et al.⁴ Significant advances in DIB understanding and applications have been reported over the past 4 years on DIB characteristics,^{5–7} functional networks^{8–10} (screening pore blockers, light sensing, biobattery), asymmetric DIBs,¹¹ electronic circuits,¹² light driven motion of DIB forming droplets,¹³ external feedback control,¹⁴ mechanical means of controlling DIB,¹⁵ nanopore translocation,¹⁶ and different microfluidic approaches^{17–19} to form DIBs.

In this paper, we present results on the incorporation of photopolymerizable lipids in DIBs. Photopolymerization of

lipids in lipid bilayers dates back to the 1980s.^{20–33} This process was developed mainly to enhance the stability of lipid bilayers, more specifically for liposomes as they are typically used for drug delivery. Several comprehensive reviews of polymerizable amphiphiles and their applications have been published.^{34–38} Unlike semispherical, enclosed lipid bilayer structures such as liposomes and vesicles, the DIB is an open-ended, planar unsupported membrane. Planar membranes are typically used for transmembrane studies, such as transport of ions and molecules through various types of proteins and nanopores in the membrane. Even though polymerizable amphiphiles are extensively studied for application mainly in liposomes and vesicles, some researchers reported on their use in planar lipid bilayers. Pore insertions in bilayer membranes were recorded^{39,40} even after photopolymerization of lipids, indicating that photopolymerizable lipids enhanced membrane stability and allowed for ion channel insertions even after photopolymerization. In supported lipid bilayers, these types of lipids were mainly used for lithographic patterning,^{41,42} for studying bilayer stability,^{43,44} and for demonstrating molecules activity retention^{45,46} in the bilayer even after polymerization.

An interesting phenomenon associated with the combination of different types of lipids in bilayers is the existence of phase-separated domains.^{34,42,47} Decreasing the ratio of nonpolymerizable to polymerizable lipids in a liposome results in reduced stability.^{21,48} Recently, Yavlovich et al.⁴⁹ designed liposomes

Received: March 19, 2012

Revised: April 30, 2012



with a combination of nonpolymerizable (DPPC = 1,2-dipalmitoyl-*sn*-glycero-3-phosphocholine) and polymerizable (23:2 DiynePC = 1,2-bis(10,12-tricosadiynoyl)-*sn*-glycero-3-phosphocholine) lipids for triggered release of contents. Various combinations of regular lipids and photopolymerizable lipids were tested under different ultraviolet C (UV-C) exposure conditions and analyzed for optimum conditions for release of fluorescent molecules from their liposomes. Recently, Yavlovich et al.⁵⁰ reported the use of visible light (514 nm laser) triggered release of liposome contents, demonstrating the usefulness of this approach to *in vivo* drug delivery applications. In this work, we have adopted a lipid-mixture composition (~80 vol % DPPC and ~20 vol % 23:2 DiynePC) in our DIB that is similar to one of the best performing compositions in liposomes designed for UV-C triggered release of contents. We have also investigated DPhPC (1,2-diphytanoyl-*sn*-glycero-3-phosphocholine) as an alternative to DPPC. A schematic diagram of the DIB formation using a mixture of DPPC (or DPhPC) and 23:2 DiynePC and its electrical investigation is shown in Figure 1a. The photopolymerization of 23:2 DiynePC

nePC) were used as regular and photopolymerizable lipids (purchased from Avanti Polar Lipids, Inc.), each at 5 mg/mL in dodecane (99%, Acros Organics). Dodecane-lipid suspensions were stored in a freezer. With either "Dodecane-DPPC" or "dodecane-DPhPC", "Dodecane-23:2 DiynePC" was mixed in 4:1 by volume for experiments. DPPC and 23:2 DiynePC have rather high turbidity (milky white appearance) in dodecane. Therefore, probe sonication (Misonix S-4000) is performed prior to use to make these suspensions transparent for experiments. The temperature during sonication was less than the transition temperature of the lipids (≤ 40 °C). "Dodecane-DPhPC" is transparent, and hence, only mild sonication was done in an ultrasound sonicator (Fisher Scientific FS60H) prior to experiments.

Droplets. The "150 mM KCl-10 mM HEPES" buffer solution at neutral pH was used for droplets. Droplet volume in most of the experiments was 500 nL. For experiments involving UV-C triggered release of fluorescent contents, calcein (MS Biomedicals, LLC) was mixed in the above-mentioned buffer (1 mg/mL). Calcein is a fluorescent dye with excitation and emission wavelengths of 495 and 515 nm, respectively, at neutral pH. The net charge of calcein⁵¹ is -3.

Substrates. Rectangular channels were laser cut in acrylic sheets and epoxy bonded to thin plastic slides. These channels contained minute quantities of dodecane-lipid suspensions (≤ 200 μL) and aqueous droplets.

Experimental Setup. Experiments were carried out on the stage of a Nikon Eclipse Ti-U inverted fluorescent microscope equipped with a Nikon DS-Qi1Mc monochrome camera and NIS Elements Basic Research software. The experimental setup consisted of a microsyringe (0.5 μL, Stoelting Co.), UV-C lamp (USHIO G8T5 8W 254 nm, 115 V, 60 Hz), PicoAmp 300B BLM amplifier (Eastern Scientific, LLC) with ADA 1210 DAQ analog-to-digital converter and TracerDAQ software, 125 μm diameter Ag/AgCl wire electrodes with 5 wt % agarose coating at one of their ends, and a homemade Faraday cage. For capacitance measurements, HP 4275A LCR meter was used at 10 kHz.

DIB Formation and Recordings. Two aqueous droplets (~500 nL) were injected in a fluidic channel, filled with ~200 μL of lipid-oil (DPPC/23:2 DiynePC combination or DPhPC/23:2 DiynePC combination in 4:1 by volume), using a microsyringe. A lipid monolayer formed around each droplet. Two Ag/AgCl wire electrodes (~125 μm diameter) were used, one for each droplet. One end of each wire electrode is coated with 5 wt % agarose and inserted into each droplet. Lipid monolayer coated aqueous droplets are anchored to the hydrogel coated ends of the wire electrodes. A portion of each wire is clamped to the arm of an XYZ micromanipulator, and other end of the wire electrodes soldered to a gold plated 1 mm male pin. These gold plated pins are inserted into the headstage of a bilayer amplifier for varying voltage across DIB and for recording DIB current. By moving the manipulators' electrode arms manually, movement of each droplet inside the channel is controlled and a DIB membrane is formed at the interface of two lipid monolayer coated droplets. DIB formation is initiated 10–15 min after the injection of droplets in lipid-oil in order to allow for sufficient lipid monolayer coating around each droplet. For current versus voltage recordings (before and after UV-C exposure of DIB), the DC voltage is varied across the DIB in step increments using the bilayer amplifier. Current traces with time are recorded at each DC voltage for at least 30 s using an ADA 1210 DAQ analog-to-digital converter and TracerDAQ software. The average value of the current is then computed at each DC voltage. A home-built Faraday cage is used to minimize electrical noise during current recordings across DIB. Electrical recordings are carried out in darkroom conditions to minimize noise. Simultaneous electrical and optical recordings are performed on the DIB membranes. For UV-C exposure, a USHIO G8T5 UV-C lamp was placed on the microscope stage approximately 5 cm above the sample. Current recordings are not performed when the UV-C lamp is on because of increased noise level. After 5 min of UV-C exposure, the lamp is turned off, and electrical measurements are restarted. This procedure is repeated after additional UV-C exposures.

A HP 4275A LCR meter was used DIB capacitance measurements at 10 kHz and 100 mV rms applied voltage. Low-noise BNC cables

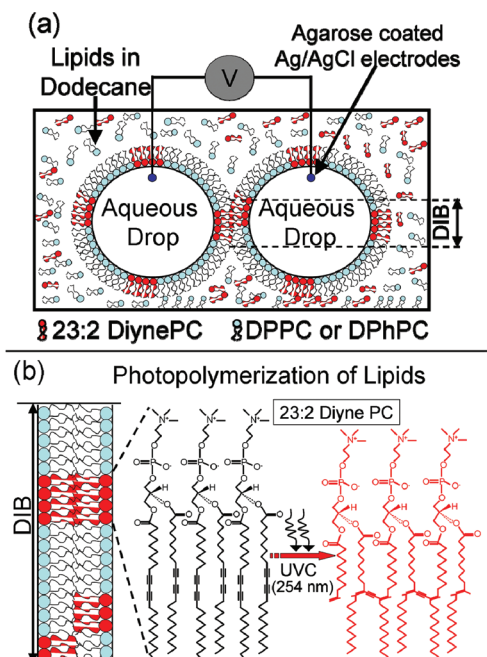


Figure 1. Schematic diagrams: (a) droplet interface bilayer (DIB) formed using a mixture of DPPC or DPhPC and 23:2 DiynePC (4:1 vol %; 5 mg/mL) in dodecane; (b) cross-linking of 23:2 DiynePC lipid domains under UV-C exposure (254 nm).

lipid domains in the DIB is shown schematically in Figure 1b. Significant changes in the current across the DIB after UV-C exposure (with a peak wavelength of 254 nm) were observed, presumably resulting from the cross-linking of the photopolymerizable lipids in DIB. Also, the transfer of encapsulated fluorescent contents (calcein) across the DIB from one drop to the other was observed after exposure to UV-C. Experimental procedure, results, and discussion are presented in the following sections.

II. EXPERIMENTAL PROCEDURE

Lipid Oil. 1,2-Dipalmitoyl-*sn*-glycero-3-phosphocholine (DPPC), 1,2-diphytanoyl-*sn*-glycero-3-phosphocholine (DPhPC), and 1,2-di-(10z,12z-tricosadiynoyl)-*sn*-glycero-3-phosphocholine (23:2 Diyne-

were used between the LCR meter and the micromanipulator arms. The DIB capacitance was recorded before and after UV–C exposure. Simultaneously, optical recordings were performed to measure the DIB lateral length and thus be able to calculate the capacitance per unit area. For analyzing the calcein leakage across the DIB, gray scale values were obtained along a line running equidistant on both sides of the DIB using the plot profile function in Image J software.

III. RESULTS

A. Characterization. The presence of photopolymerizable lipids in lipid oil was confirmed using spectrophotometer analysis. “Dodecane-DPPC” (5 mg of DPPC/1 mL of dodecane) and “Dodecane-23:2 DiynePC” (5 mg of 23:2 DiynePC/1 mL of dodecane), prepared in two different vials, are mixed in 4:1 ratio by volume. From that mixture, a 2 μ L volume was placed in the Nanodrop 1000 apparatus (Thermo Scientific), and absorbance was recorded across a range of wavelengths. Spectra showing optical absorbance versus wavelength are shown in Figure 2a. An increase in absorbance

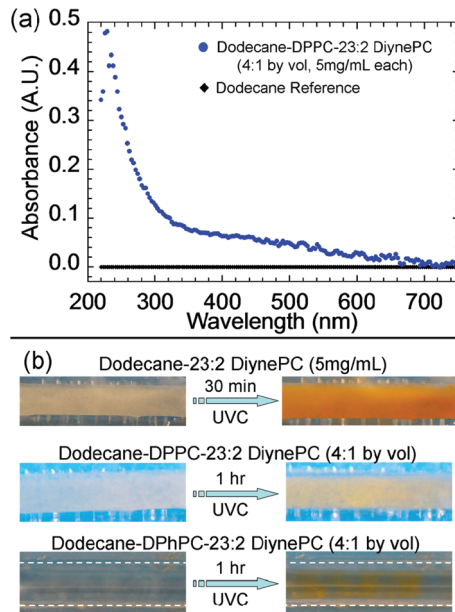


Figure 2. Characterization of photopolymerizable lipids in dodecane-lipid medium: (a) Spectrophotometer's absorbance versus wavelength for “Dodecane-DPPC-23:2 DiynePC” (4:1 by vol, 5 mg/mL each) sample; (b) color change of “Dodecane-23:2 DiynePC”, “Dodecane-DPPC-23:2 DiynePC”, and “Dodecane-DPhPC-23:2 DiynePC” after UV–C exposure.

was observed at UV–C wavelengths (close to 254 nm), which is an indication of the presence of monomeric 23:2 DiynePC. A dodecane only sample is used as reference for measurements. Another characteristic of photopolymerization of 23:2 DiynePC lipids is the color change to red after UV–C exposure. This was observed by exposing a channel filled with ~200 μ L to UV–C lamp using dodecane solutions with photopolymerizable lipids (23:2 DiynePC) only or solutions with 4:1 by volume ratio of nonphotopolymerizable (DPPC or DPhPC) to polymerizable lipids. Figure 2b shows respective channel images before and after UV–C exposure. As expected, the strongest color change to red occurs in the sample with highest 23:2 DiynePC concentration.

The resistance of the DIB was calculated based on average current (I) versus DC voltage (V) response. For this, 500 nL

“150 mM KCl–10 mM HEPES” droplets were used to form different DIBs with DPPC-23:2 DiynePC (4:1 by vol) and with DPhPC-23:2 DiynePC (4:1 by vol). The voltage across each DIB was increased in 20 mV increments. At each DC voltage, current traces were recorded with time. The average current at each voltage was then calculated using the current trace data. I – V characteristics for two different DIBs (DIB#1 and DIB#2) formed with “DPPC-23:2 DiynePC” and “DPhPC-23:2 DiynePC” are shown in Figure 3a and b, respectively. The DIB resistance was typically in the range of 3–10 G Ω .

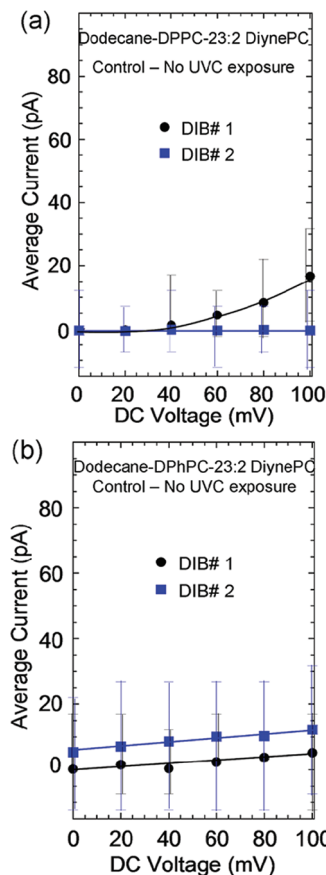


Figure 3. Plot of average current magnitude versus DC voltage under negative bias in the absence of UV–C exposure for different DIBs formed with (a) DPPC-23:2 DiynePC (4:1 by vol); (b) DPhPC-23:2 DiynePC (4:1 by vol).

The DIB capacitance was measured before and after UV–C exposure. The capacitance is recorded vs time while a DIB is formed between two 1 μ L “150 mM KCl–10 mM HEPES” droplets in “Dodecane-DPhPC-23:2 DiynePC” solution at 100 mV rms 10 kHz. As shown in Figure 4a, before DIB formation, there is no significant capacitance measured. As soon as the DIB is formed, the applied voltage is dropped across the lipid bilayer and the capacitance suddenly increased and then stabilized with time. To illustrate the stability of the DIB with UV–C exposure, after initial measurement, the droplets are separated and exposed to UV–C for 15 min. The DIB is then reformed after UV–C exposure and the capacitance is remeasured. The lateral DIB dimension was measured using the optical microscope. As aqueous drops are not ideally spherical on flat substrates, an elliptical area is assumed for DIB area with minor axis as half of major axis (lateral DIB

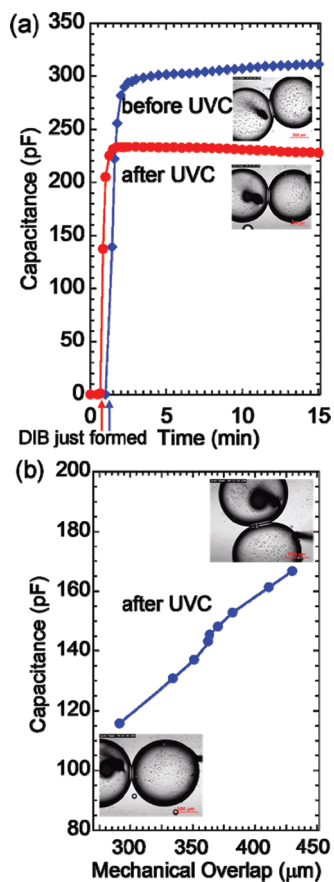


Figure 4. DIB capacitance at 100 mV rms 10 kHz across 1 μL “150 mM KCl-10 mM HEPES” drops in “Dodecane-DPhPC-23:2 DiynePC” (4:1 by vol, 5 mg/mL each): (a) capacitance versus time before and after UV-C exposure; (b) capacitance versus mechanical overlap.

dimension). Specific capacitance is calculated by dividing recorded capacitance at a given time by DIB area at that time. As can be seen in Figure 4a, the DIB capacitance after UV-C exposure is stable with time. The difference in the steady state capacitance value is due to the difference in DIB dimension. At 15 min measurement, the measured DIB capacitance values before and after UV-C exposure are 311.3 and 227.6 pF, respectively. The corresponding DIB lateral dimension before and after UV-C exposure are 439 and 377 μm , respectively. This results in nearly equal calculated specific capacitances before and UV-C exposure of $\sim 0.41 \mu\text{F}/\text{cm}^2$, which is in reasonable agreement⁴ with reported specific capacitances of artificial lipid bilayers. This indicates that the lipid bilayer is in stable condition even after UV-C exposure.

The mechanical stability of the lipid membrane is tested by forming the DIB with minimum droplet interface and then manually pressing droplets toward each other using electrodes that are attached to micromanipulators, thereby increasing DIB lateral dimension. If the lipid membrane is weak, the DIB would break immediately as DIB drops are pushed toward each other. In general, we observed good stability of DIB even at larger DIB lateral dimensions. An example is shown in Figure 4b, where the capacitance of a UV-C exposed DIB is seen to increase linearly as DIB lateral dimension was mechanically increased. Typical error in measuring the DIB lateral dimension in the microscope is of the order of a few ($\sim 1\text{--}3$) micrometers.

B. Effect of UV-C Exposure on DIB Conduction. The 500 nL “150 mM KCl-10 mM HEPES” drops are dispensed in “Dodecane-DPPC-23:2 DiynePC”. Agarose coated (5 wt % in DI water) Ag/AgCl electrodes were inserted into the droplets. DIB was formed, and current traces (with time) were recorded at different DC voltages before UV-C exposure, after 5 min of UV-C exposure, and after an additional 5 min of UV-C exposure. A plot of average current versus DC voltage is shown in Figure 5. It is important to note that there is negligible

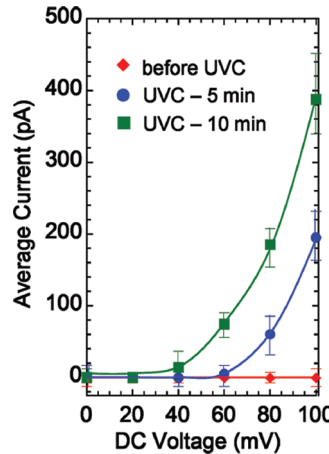


Figure 5. Plot of average current magnitude versus DC voltage under negative bias in the presence of UV-C exposure for a DIB formed with 500 nL “150 mM KCl-10 mM HEPES” drops in “Dodecane-DPPC-23:2 DiynePC” (4:1 by vol, 5 mg/mL each).

current prior to UV-C exposure. As the UV-C exposure time was increased from 5 to 10 min, the current across the DIB increased at all voltages. This indicates that photopolymerizable lipid domains in DIB have cross-linked and have shrunk in size,^{35,52,53} resulting in pores between lipid domains in the DIB. Changes in current with exposure to white light of microscope are minimum (see Figure 3a) when compared to that of UV-C exposure. This confirms that UV-C has a dominant effect on cross-linking of photopolymerizable lipids and pore formation in DIB.

C. Release of Droplet-Encapsulated Contents in DIB after UV-C Exposure. A potential application of having photopolymerizable lipids in DIB is the triggered release of encapsulated contents in droplets across the DIB. If porosity arises in the DIB lipid membrane due to cross-linking of photopolymerizable lipids upon UV-C exposure, then contents in one droplet should diffuse through the pores generated in the DIB to the other droplet. A schematic diagram of this application is shown in Figure 6. To demonstrate this effect, calcein was encapsulated in a droplet at a concentration of 1 mg/mL in “150 mM KCl-10 mM HEPES”. Only one of the two DIB forming droplets was loaded with calcein at the beginning of the experiment. DIB was formed and observed with time, while fluorescence microscopic images of the DIB along with the droplets in the channel were simultaneously observed. Control experiments, with no UV-C exposure, yielded no significant release of calcein across the DIB. We observed significant release of calcein with time across DIB from one drop to another upon UV-C exposure. This passive release of calcein across the DIB is due to the pores formed in DIB during the photopolymerization of 23:2 DiynePC. To increase calcein diffusion rate (active diffusion) and to ensure

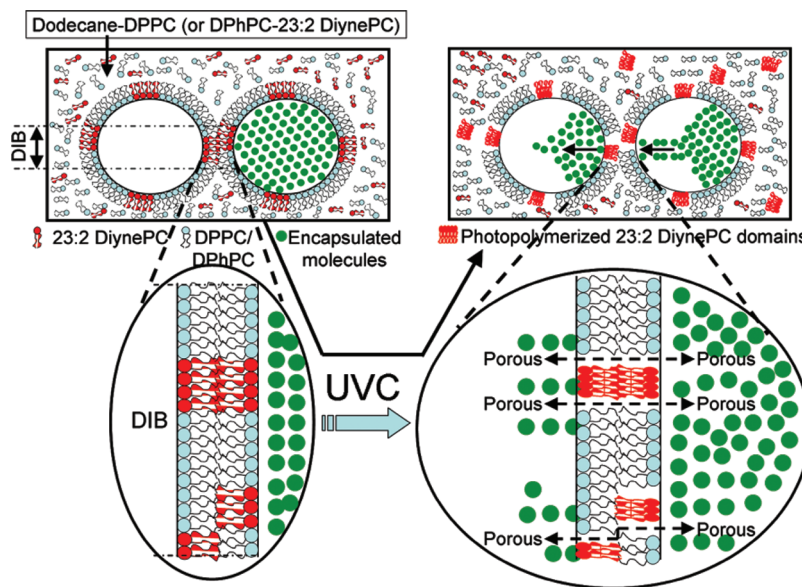


Figure 6. Schematic diagram showing the mechanism behind the UV-C triggered release of encapsulated contents of a drop across DIB that is formed with a mixture of DPPC or DPhPC and 23:2 DiynePC in dodecane.

that the DIB is intact (electrocompression), a DC voltage was applied across the DIB during the UV-C exposure in some experiments. To confirm that calcein diffusion across DIB does not occur due to any inherent membrane porosity and the applied voltage, control experiments were performed with voltage but no UV-C exposure. In those cases, only minimal release of calcein across the DIB was observed. This indicates that DC voltage by itself is not sufficient to produce diffusion across the DIB membrane in the absence of UV-C exposure. Significant calcein release was observed only during UV-C exposure. Results of triggered calcein release with DPhPC-23:2 DiynePC (4:1 by vol) in DIB are shown in Figure 7. Results of triggered calcein release with DPPC-23:2 DiynePC (4:1 by vol) in DIB are shown in Figure S1 of the Supporting Information. For Figures 7a and S1a, plot profile function of ImageJ software (NIH) was used to quantify changes in fluorescence associated with calcein diffusion into the second droplet as a function of time. Gray values were measured on microscopic fluorescent images to a distance of 250 μm on either side of the DIB along a line intersecting the DIB and extending equally into both droplets. The percent of calcein in the left droplet is relative to the amount of calcein present in the right droplet, both at a distance of 250 μm from the DIB. Microscopic images in Figures 7b and S1b show DIBs along with droplets at different relative times under different experimental conditions. Another parameter of interest is droplet shape. In general, the droplet shape can vary with time depending on the medium surrounding it. In the case of DPhPC/23:2 DiynePC combinations, the lipid-oil is initially transparent and remained transparent during experiments. No significant changes in droplet shape with time were observed in this case. However, in the case of DPPC/23:2 DiynePC combinations, the lipid-oil was turbid (milky white) before experiment. A mild sonication was performed (with temperatures below the transition temperature) prior to experiment to make this lipid-oil transparent for microscopic imaging. However, the DPPC/23:2 DiynePC lipid-oil does return slowly to the turbid state during the experiment. This turbidity change resulted in slight droplet shape change with time in the case of DPPC/23:2

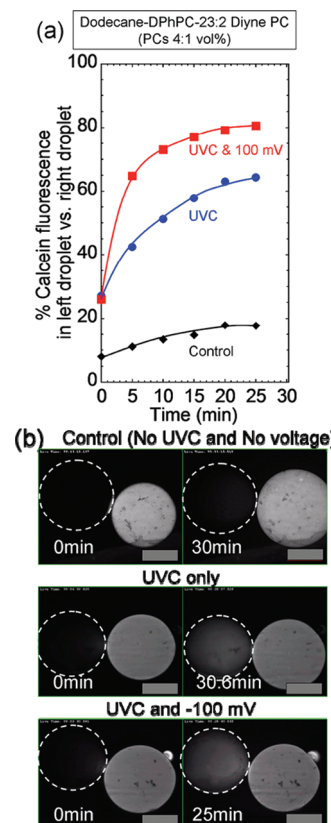


Figure 7. UV-C triggered release of calcein from right drop to left drop across DIB formed with "Dodecane-DPhPC-23:2 DiynePC" (4:1 by vol, 5 mg/mL each): (a) plot showing percentage of calcein versus time in left droplet with respect to the right drop's calcein for different experimental conditions at a distance of 250 μm from DIB; (b) fluorescence microscopic images of DIBs and droplets in channel with relative times for different experimental conditions (dark areas imply no calcein, and bright white areas show presence of calcein).

DiynePC combinations. However, turbidity changes and droplet shape changes were not significant during the time of

experiments and did not cause difficulties with simultaneous electrical and optical recordings.

IV. DISCUSSION

In this section, the effects of 23:2 DiynePC photopolymerization in DIB are discussed and compared with that in liposomes. As was described in the previous section, with UV-C exposure, 23:2 DiynePC domains in DIB are polymerized, leading to an increase in DIB membrane permeability presumably due to an increase in porosity. Photopolymerization of 23:2 DiynePC domains that are present in a significantly smaller proportion compared to DPhPC or DPPC does not change the specific capacitance of the lipid bilayer membrane. The DIB capacitance measurements with time, before and after UV-C exposure, showed a consistent specific capacitance that is in reasonable agreement with reported values for other model lipid bilayers. Also, photopolymerization of 23:2 DiynePC domains, present in limited proportion, does not result in large pores and does not make the membrane mechanically weak. This was evident from the capacitance versus DIB lateral dimension measurements where DIB capacitance increased as the DIB dimension was increased using micromanipulators. Droplets did not fuse even at larger DIB lateral dimensions, indicating that the DIB membrane is mechanically robust.

With some photopolymerizable lipids present in the DIB, current versus voltage recordings showed an increase in current across DIB after UV-C exposure, indicating that the DIB membrane became more permeable after UV-C exposure. This increase in permeability indicates that the membrane became relatively more porous with UV-C exposure. It has been shown^{21,40} that bilayer membranes or vesicles formed with photopolymerizable lipids display an increase in membrane stability. However, in the conditions used here, the photopolymerizable lipids are in relatively lower concentration in the bilayer membrane and, thus, local polymerization can occur in phase-separated domains. This will result in membrane porosity and an increase of permeability. It is important to point out that, in the case of DIB with DPPC lipids, there was always breakage of the DIB lipid membrane (droplet fusion) upon UV-C exposure. This DPPC lipid based DIB breakage was not instantaneous upon turning on the UV-C source. Droplet fusion occurred after some period of exposure, as shown in Figure S1. Before breakage, there was no leakage of calcein across DIB. Upon breakage, calcein diffusion occurred rapidly, as indicated by a spike in the corresponding plots in Figure S1a. Calcein leakage data after DIB breakage was obtained using the ImageJ plot profile function on the microscopic images. When DIB breakage happened for the "UVC only" case in Figure S1, fluorescent microscopic images were not available as the microscope was in bright field light mode during the breakage time. Hence, for the Figure S1 "UV-C only" case, a dotted line is shown. However, in the case of DIB with DPhPC lipids, the DIB lipid membrane did not break upon UV-C exposure and a time release of calcein was observed. It is believed that this is because of the additional membrane stability offered by the structure of DPhPC.

There are certain differences between a triggered release of liposomal contents versus a release across a DIB. In the case of liposomes that are three-dimensional and semispherical, the entire encapsulated contents release into the surrounding aqueous medium immediately as soon as a small break occurs at any point on the liposome surface. In addition, individual liposomal release is not normally monitored, as typically a

group of liposomes are experimented in a vial or a well-plate. In the case of DIBs, leakage conditions are focused on a defined planar lipid membrane area. In DIB, the surrounding medium for droplets is a dodecane-lipid mixture. The release of water-soluble encapsulates from the loaded aqueous droplet will preferentially occur to the virgin aqueous droplet through the pores generated in the defined DIB lipid membrane area.

Specific advantages of using the DIB approach for drug-delivery *in vitro* studies are the simplicity and flexibility in using DIBs. The DIB approach uses minute quantities of aqueous droplets (picoliters to nanoliters to microliters) and of assorted dodecane-lipid combinations ($\leq 200 \mu\text{L}$). It is also very simple to form the desired alkane-lipid mixtures. There are also some limitations to the use of the DIB approach. DIBs are intended only for *in vitro* studies, while liposomes can eventually be used for *in vivo* applications. Another limitation in DIB-based studies is material compatibility. Some lipids do not suspend well in dodecane, resulting in turbidity. This causes difficulties in visualizing the aqueous droplets by microscope, as well as in maintaining good droplet shape with time inside the dodecane-lipid medium. However, before investing time and resources on new experiments involving radiation based release of liposomal contents, it is worth using the DIB approach as a relatively simple and fast method to determine if the compounds are sufficiently promising to warrant investigation using liposomes. In terms of future DIB experiments, it will be interesting to experiment with different types and proportions of photopolymerizable and nonphotopolymerizable lipids in DIB. Also, based on a recent report by Yavlovich et al. (ref 53), it will be interesting to observe the effects of various wavelengths in the visible range on DIBs containing certain photopolymerizable lipids.

V. SUMMARY AND CONCLUSIONS

DIB lipid membranes are formed using a mixture of DPPC or DPhPC (nonpolymerizable) and 23:2 DiynePC (polymerizable) in 4:1 by volume in dodecane (5 mg/mL each). 23:2 DiynePC domains in DIB were cross-linked by exposure to UV-C. Photopolymerization of 23:2 DiynePC in dodecane-lipid medium was confirmed using spectrophotometer analysis and color changes after UV-C exposure. DIB electrical resistance is in the 3–10 G Ω range in the absence of UV-C exposure. In the presence of white light, the DIB conductivity varied only slightly. With exposure to UV-C, the DIB conductivity increased significantly, indicating that cross-linking in domains of 23:2 DiynePC due to photopolymerization is resulting in a porous DIB membrane. Release of encapsulated fluorescent contents (calcein) from the loaded droplet to the virgin droplet across the DIB upon UV-C exposure was observed using fluorescence microscopy. These results indicate that it is possible to control DIB porosity with UV-C exposure when the lipid bilayer membrane contains photopolymerizable lipids. In conclusion, DIB offers a simple and flexible platform for investigating various *in vitro* phenomena.

■ ASSOCIATED CONTENT

S Supporting Information

Additional figure showing UV-C triggered release of calcein. This material is available free of charge via the Internet at <http://pubs.acs.org>.

AUTHOR INFORMATION

Corresponding Author

*E-mail: a.steckl@uc.edu.

Notes

The authors declare no competing financial interest.

REFERENCES

- (1) Edidin, M. Lipids on the frontier: a century of cell-membrane bilayers. *Na. Rev. Mol. Cell Biol.* **2003**, *4*, 414–418.
- (2) Tien, H. T.; Ottova, A. L. The lipid bilayer concept and its experimental realization: from soap bubbles, kitchen sink, to bilayer lipid membranes. *J. Membr. Sci.* **2001**, *189*, 83–117.
- (3) Tsوفина, Л. М.; Либерман, Е. А.; Бабаков, А. В. Production of bimolecular protein-lipid membranes in aqueous solution. *Nature* **1966**, *212*, 681–683.
- (4) Funakoshi, K.; Suzuki, H.; Takeuchi, S. Lipid Bilayer Formation by Contacting Monolayers in a Microfluidic Device for Membrane Protein Analysis. *Anal. Chem.* **2006**, *78*, 8169–8174.
- (5) Hwang, W. L.; Holden, M. A.; White, S.; Bayley, H. Electrical Behavior of Droplet Interface Bilayer Networks: Experimental Analysis and Modeling. *J. Am. Chem. Soc.* **2007**, *129*, 11854–11864.
- (6) Punnamaraju, S.; Steckl, A. J. Voltage Control of Droplet Interface Bilayer Lipid Membrane Dimensions. *Langmuir* **2011**, *27*, 618–626.
- (7) Thutupalli, S.; Herminghaus, S.; Seemann, R. Bilayer membranes in micro-fluidics: from gel emulsions to soft functional devices. *Soft Matter* **2011**, *7*, 1312–1320.
- (8) Holden, M. A.; Needham, D.; Bayley, H. Functional Bionetworks from Nanoliter Water Droplets. *J. Am. Chem. Soc.* **2007**, *129*, 8650–8655.
- (9) Bayley, H.; Cronin, B.; Heron, A.; Holden, M. A.; Hwang, W. L.; Syeda, R.; Thompson, J.; Wallace, M. Droplet interface bilayers. *Mol. BioSyst.* **2008**, *4*, 1191–1208.
- (10) Xu, J.; Sigworth, F. J.; Lavan, D. A. Synthetic Protocells to Mimic and Test Cell Function. *Adv. Mater.* **2009**, *21*, 1–8.
- (11) Hwang, W. L.; Chen, M.; Cronin, B.; Holden, M. A.; Bayley, H. Asymmetric Droplet Interface Bilayers. *J. Am. Chem. Soc.* **2008**, *130*, 5878–5879.
- (12) Maglia, G.; Heron, A. J.; Hwang, W. L.; Holden, M. A.; Mikhailova, E.; Li, Q.; Cheley, S.; Bayley, H. Droplet networks with incorporated protein diodes show collective properties. *Nat. Nanotechnol.* **2009**, *4*, 437–440.
- (13) Dixit, S. S.; Kim, H.; Vasilyev, A.; Eid, A.; Faris, G. W. Light-Driven Formation and Rupture of Droplet Bilayers. *Langmuir* **2010**, *26*, 6193–6200.
- (14) Sarles, S. A.; Leo, D. J. Tailored Current-Voltage Relationships of Droplet-Interface Bilayers Using Biomolecules and External Feedback Control. *J. Intell. Mater. Syst. Struct.* **2009**, *20*, 1233–1247.
- (15) Sarles, S. A.; Leo, D. J. Physical encapsulation of droplet interface bilayers for durable, portable biomolecular networks. *Lab Chip* **2010**, *10*, 710–717.
- (16) Renner, S.; Geltlinger, S.; Simmel, F. C. Nanopore Translocation and Force Spectroscopy Experiments in Microemulsion Droplets. *Small* **2010**, *6*, 190–194.
- (17) Stanley, C. E.; Elvira, K. S.; Niu, X. Z.; Gee, A. D.; Ces, O.; Edel, J. B.; deMello, A. J. A microfluidic approach for high-throughput droplet interface bilayer (DIB) formation. *Chem. Commun.* **2010**, *46*, 1620–1622.
- (18) Aghdaei, S.; Sandison, M. E.; Zagnoni, M.; Green, N. G.; Morgan, H. Formation of artificial lipid bilayers using droplet dielectrophoresis. *Lab Chip* **2008**, *8*, 1617–1620.
- (19) Poulos, J. L.; Nelson, W. C.; Jeon, T.-J.; Kim, C.-J.; Schmidt, J. J. Electrowetting on dielectric-based microfluidics for integrated lipid bilayer formation and measurement. *Appl. Phys. Lett.* **2009**, *95*, 013706–1–013706–3.
- (20) Johnston, D. S.; Sanghera, S.; Pons, M.; Chapman, D. Phospholipid Polymers - Synthesis and Spectral Characteristics. *Biochim. Biophys. Acta* **1980**, *602*, 57–69.
- (21) Regen, S. L.; Singh, A.; Oehme, G.; Singh, M. Polymerized Phosphatidyl Choline Vesicles: Stabilized and Controllable Time-Release Carriers. *Biochem. Biophys. Res. Commun.* **1981**, *101*, 131–136.
- (22) Lopez, E.; O'Brien, D. F.; Whitesides, T. H. Effects of Membrane Composition and Lipid Structure on the Photopolymerization of Lipid Diacetylenes in Bilayer Membranes. *Biochim. Biophys. Acta* **1982**, *693*, 437–443.
- (23) Regen, S. L.; Singh, A.; Oehme, G.; Singh, M. Polymerized Phosphatidylcholine Vesicles: Synthesis and Characterization. *J. Am. Chem. Soc.* **1982**, *104*, 791–795.
- (24) Hupfer, B.; Ringsdorf, H.; Schupp, H. Liposomes from Polymerizable Phospholipids. *Chem. Phys. Lipids* **1983**, *33*, 355–374.
- (25) Leaver, J.; Alonso, A.; Durrani, A. A.; Chapman, D. The Physical Properties and Photopolymerization of Diacetylene-containing Phospholipid Liposomes. *Biochim. Biophys. Acta* **1983**, *732*, 210–218.
- (26) Hayward, J. A.; Chapman, D. Biomembrane surfaces as models for polymer design: the potential for haemocompatibility. *Biomaterials* **1984**, *5*, 135–142.
- (27) Hayward, J. A.; Johnston, D. S.; Chapman, D. Polymeric Phospholipids as New Biomaterials. *Ann. N.Y. Acad. Sci.* **1985**, *446*, 267–281.
- (28) Hayward, J. A.; Levine, D. M.; Neufeld, L.; Simon, S. R.; Johnston, D. S.; Chapman, D. Polymerized liposomes as stable oxygen-carriers. *FEBS Lett.* **1985**, *187*, 261–266.
- (29) O'Brien, D. F.; Klingbiel, R. T.; Specht, D. P.; Tyminski, P. N. Preparation and Characterization of Polymerized Liposomes. *Ann. N.Y. Acad. Sci.* **1985**, *446*, 282–295.
- (30) Regen, S. L. Polymerized Phosphatidylcholine Vesicles as Drug Carriers. *Ann. N.Y. Acad. Sci.* **1985**, *446* (1), 296–307.
- (31) Sadownik, A.; Stefely, J.; Regen, S. L. Polymerized Liposomes Formed under Extremely Mild Conditions. *J. Am. Chem. Soc.* **1986**, *108*, 7789–7791.
- (32) Georger, J. H.; Singh, A.; Price, R. R.; Schnur, J. M.; Yager, P.; Schoen, P. E. Helical and Tubular Microstructures Formed by Polymerizable Phosphatidylcholines. *J. Am. Chem. Soc.* **1987**, *109*, 6169–6175.
- (33) Rhodes, D. G.; Blechner, S. L.; Yager, P.; Schoen, P. E. Structure of polymerizable lipid bilayers. I-1,2-bis(10,12-tricosadiynoyl)-sn-glycero-3-phosphocholine, a tubule-forming phosphatidylcholine. *Chem. Phys. Lipids* **1988**, *49*, 39–47.
- (34) Armitage, B.; Bennett, D. E.; Lamparski, H. G.; O'Brien, D. F. Polymerization and Domain Formation in Lipid Assemblies. *Adv. Polym. Sci.* **1996**, *126*, 53–84.
- (35) Shum, P.; Kim, J.-M.; Thompson, D. H. Phototriggering of liposomal drug delivery systems. *Adv. Drug Delivery Rev.* **2001**, *53*, 273–284.
- (36) Mueller, A.; O'Brien, D. F. Supramolecular Materials via Polymerization of Mesophases of Hydrated Amphiphiles. *Chem. Rev.* **2002**, *102*, 727–757.
- (37) Andrensen, T. L.; Jensen, S. S.; Jorgensen, K. Advanced strategies in liposomal cancer therapy: Problems and prospects of active and tumor specific drug release. *Prog. Lipid Res.* **2005**, *44*, 68–97.
- (38) Zhang, H.; Joubert, J. R.; Saavedra, S. S. Membranes from Polymerizable Lipids. *Adv. Polym. Sci.* **2010**, *224*, 1–42.
- (39) Shenoy, D. K.; Barger, W. R.; Singh, A.; Panchal, R. G.; Misakian, M.; Stanford, V. M.; Kasianowicz, J. J. Functional Reconstitution of Protein Ion Channels into Planar Polymerizable Phospholipid Membranes. *Nano Lett.* **2005**, *5*, 1181–1185.
- (40) Daly, S. M.; Heffernan, L. A.; Barger, W. R.; Shenoy, D. K. Phopolymerization of Mixed Monolayers and Black Lipid Membranes Containing Gramicidin A and Diacetylenic Phospholipids. *Langmuir* **2006**, *22*, 1215–1222.
- (41) Morigaki, K.; Baumgart, T.; Offenhausser, A.; Knoll, W. Patterning Solid-Supported Lipid Bilayer Membranes by Lithographic Polymerization of a Diacetylene Lipid. *Angew. Chem., Int. Ed.* **2001**, *40*, 172–174.
- (42) Okazaki, T.; Tatsu, Y.; Morigaki, K. Phase Separation of Lipid Microdomains Controlled by Polymerized Lipid Bilayer Matrices. *Langmuir* **2010**, *26*, 4126–4129.

- (43) Ross, E. E.; Bondurant, B.; Spratt, T.; Conboy, J. C.; O'Brien, D. F.; Saavedra, S. S. Formation of Self-Assembled, Air-Stable Lipid Bilayer Membranes on Solid Supports. *Langmuir* **2001**, *17*, 2305–2307.
- (44) Conboy, J. C.; Liu, S.; O'Brien, D. F.; Saavedra, S. S. Planar Supported Bilayer Polymers Formed from Bis-Diene Lipids by Langmuir-Blodgett Deposition and UV Irradiation. *Biomacromolecules* **2003**, *4*, 841–849.
- (45) Subramaniam, V.; Alves, I. D.; Salgado, G. F. J.; Lau, P.-W.; Wysocki, R. J., Jr.; Salamon, Z.; Gordon, T.; Hruby, V. J.; Brown, M. F.; Saavedra, S. S. Rhodopsin Reconstituted into a Planar-Supported Lipid Bilayer Retains Photoactivity after Cross-Linking of Lipid Monomers. *J. Am. Chem. Soc.* **2005**, *127*, 5320–5321.
- (46) Michel, R.; Subramaniam, V.; McArthur, S. L.; Bondurant, B.; D'Ambruoso, G. D.; Hall, H. K., Jr.; Brown, M. F.; Ross, E. E.; Saavedra, S. S.; Castner, D. G. Ultra-High Vacuum Surface Analysis Study of Rhodopsin Incorporation into Supported Lipid Bilayers. *Langmuir* **2008**, *24*, 4901–4906.
- (47) Temprana, C. F.; Duarte, E. L.; Taira, M. C.; Lamy, M. T.; Alonso, S. d. V. Structural Characterization of Photopolymerizable Binary Liposomes Containing Diacetylenic and Saturated Phospholipids. *Langmuir* **2010**, *26*, 10084–10092.
- (48) Bondurant, B.; O'Brien, D. F. Photoinduced Destabilization of Sterically Stabilized Liposomes. *J. Am. Chem. Soc.* **1998**, *120*, 13541–13542.
- (49) Yavlovich, A.; Singh, A.; Tarasov, S.; Capala, J.; Blumenthal, R.; Puri, A. Design of liposomes containing photopolymerizable phospholipids for triggered release of contents. *J. Therm. Anal. Calorim.* **2009**, *98*, 97–104.
- (50) Yavlovich, A.; Singh, A.; Blumenthal, R.; Puri, A. A novel class of photo-triggerable liposomes containing DPPC:DC8,9PC as vehicles for delivery of doxorubicin to cells. *Biochim. Biophys. Acta* **2011**, *1808*, 117–126.
- (51) Oncel, M.; Khoobehi; Peyman, G. A. Calcein angiography: a preliminary report on an experimental dye. *Int. Ophthalmol.* **1990**, *14*, 245–250.
- (52) Puri, A.; Loomis, K.; Smith, B.; Lee, J.-H.; Yavlovich, A.; Heldman, E.; Blumenthal, R. Lipid-Based Nanoparticles as Pharmaceutical Drug Carriers: From Concepts to Clinic. *Crit. Rev. Ther. Drug Carrier Syst.* **2009**, *26*, 523–580.
- (53) Yavlovich, A.; Smith, B.; Gupta, K.; Blumenthal, R.; Puri, A. Light-sensitive lipid-based nanoparticles for drug delivery: design principles and future considerations for biological applications. *Mol. Membr. Biol.* **2010**, *27*, 364–381.